

Proposed design for a new borehole elastic imaging tool

Robert R. Stewart and Carlos E. Nieto

ABSTRACT

This paper proposes a new borehole televiewer device that uses short-spaced, multioffset receivers to measure an angle-versus-offset (AVO) response of the borehole wall. Using various values for the borehole fluid and elastic formation, we find significant response at critical angle and measurable AVO variation. We propose a simple tool design to capture this information. With the critical angle of the reflectivity as well as the AVO response, we could calculate the formation P- and S-velocities.

INTRODUCTION

It is useful to be able to make an image of the inside of a wellbore. Such an image can give us information about the formation dips and fractures as intersected by the borehole. Borehole televiewers or imaging tools typically have an ultrasonic transducer (about 500 kHz) that acts as a source and receiver (Figure 1). The source is pulsed into the borehole fluid and a compressional reflection is returned from the borehole wall.



Figure 1. Schlumberger borehole imaging unit. The cylindrical ultrasonic transducer acts as a source and receiver. It rotates to provide complete circumferential coverage of the borehole wall (from www.slb.com).

The transducer rotates in the tool to provide full azimuthal coverage of the borehole wall. The echo return has an amplitude that, when posted with all of the other data from around the borehole, gives an interpretable picture of the geology as

intersected by the borehole. The televiwer image is a measure of the P-wave reflectivity and rugosity of the area covered by the transmitted pulse. While a useful product on its own, we ask whether more could be determined from such a measurement? In particular, could we ascertain more petrophysical descriptors of the formation? We may well be able to do this if we enhance the simple coincident source-receiver transducers with additional receivers. The basic idea suggested here is to employ multiple acoustic detectors a short distance from the source to receive an angular distribution of the reflected signal (Figure 2). The variation of this reflection with offset can be analysed with a type of AVO methodology. In this paper, we investigate the possibility of an elastic borehole imager using up to 10 receivers plus one or two sources.

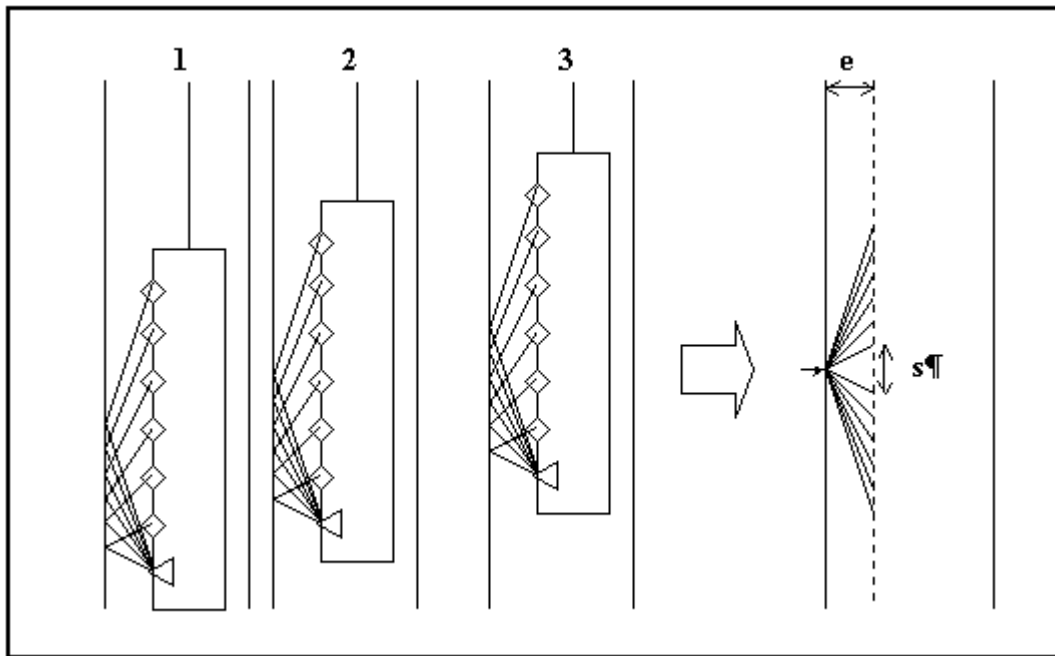


Figure 2. Schematic diagram of the basic tool design showing an acoustic source and six offset receivers (s is the offset to the first receiver, e is the distance from the tool to the borehole wall). Reflections recorded at different tool positions and offsets can be gathered about a common reflection point for further analysis.

METHODS

We first attempt to understand part of the borehole problem by using straightforward planar interface Zoeppritz equations. To that end, we have calculated the theoretical reflection coefficients for different values of velocity and density in both the borehole fluid (Table 1) and formation. We have analysed geometries approximately that of standard wells and tool – that is tool-borehole distances from 1 cm to 10 cm. We calculated responses with receiver intervals from millimetres to several centimetres (Figure 3). From the analysis of these reflectivity curves, we obtained an optimal range of angles of incidence to be sampled with the tool, i.e. those angles up to the value of the critical angle for each case.

Sample	Fluid density [kg/m ³]	Sound Velocity [m/s]	Acoustic Impedance	Sound Attenuation at 250 kHz [dB/cm]
1	1222	1389	1.69	2.25
2	1177	1250	1.47	1.30
3	1632	1219	1.99	7.25
4	1172	1316	1.54	2.30

Table 1. Acoustic properties from four drilling muds (courtesy of Baker-Hughes /Western Atlas).

Some different models are shown in Figures 4 through 7. The ray tracing results in Figure 7 are courtesy of Pat Daley. We note in these simple examples that there is significant AVO variation.

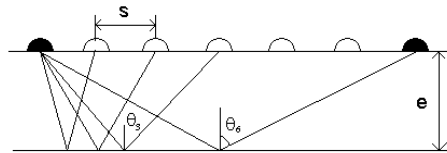


Figure 3. Schematic diagram of the source-receiver geometry and the borehole wall.

The angle of incidences are calculated from the tool and borehole geometry as:

$$\theta_1 = \tan^{-1}\left(\frac{S}{2e}\right)$$

$$\theta_2 = \tan^{-1}\left(\frac{S}{e}\right)$$

$$\theta_3 = \tan^{-1}\left(\frac{3S}{2e}\right)$$

⋮

$$\theta_n = \tan^{-1}\left(\frac{nS}{2e}\right)$$

where

n = number of receivers

S = separation between receivers

E = separation between tool and borehole wall

θ_n = angle of incidence for the nth receiver.

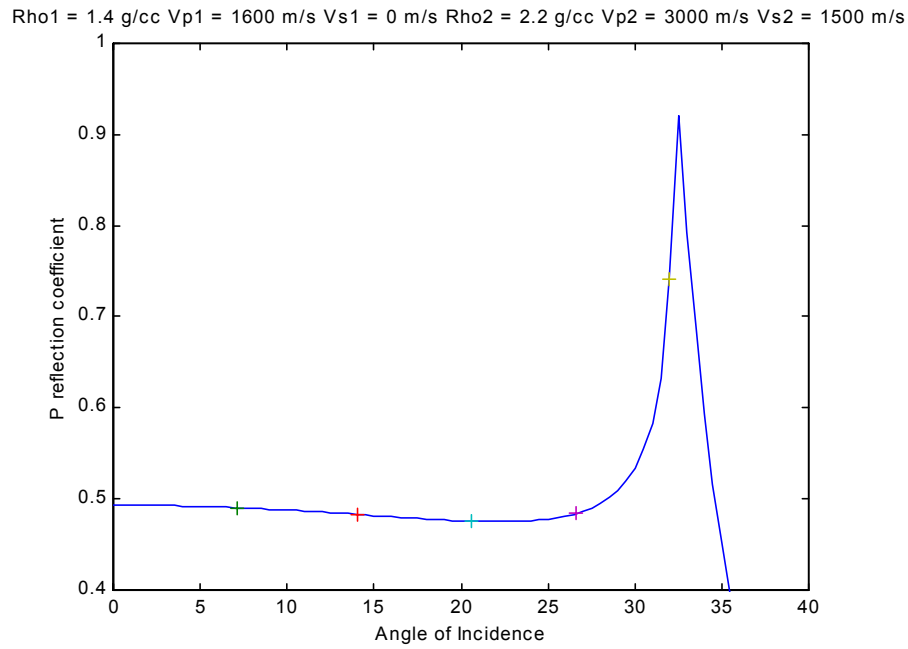


Figure 4. P reflection coefficient for a fluid on elastic solid model with fluid values ($V_{P1} = 1600$ m/s, $V_{S1} = 0$ m/s, $\rho_1 = 1.4$ g/cm³) and solid values ($V_{P2} = 3000$ m/s, $V_{S2} = 1500$ m/s, $\rho_2 = 2.2$ g/cm³).

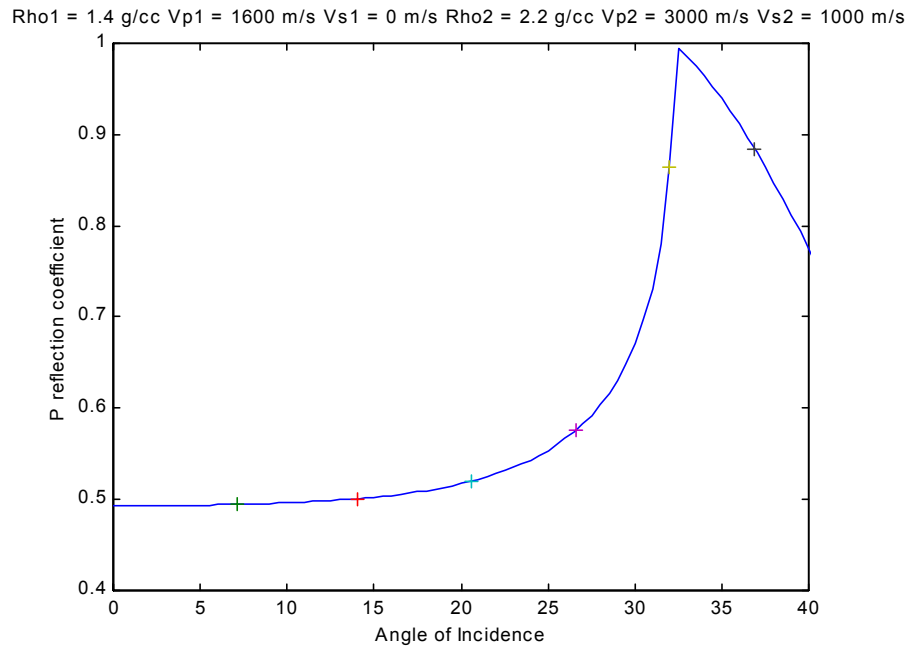


Figure 5. P reflection coefficient for a model with $V_{P1} = 1600$ m/s, $V_{S1} = 0$ m/s, $\rho_1 = 1.4$ g/cm³ and solid values of $V_{P2} = 3000$ m/s, $V_{S2} = 1000$ m/s, $\rho_2 = 2.2$ g/cm³.

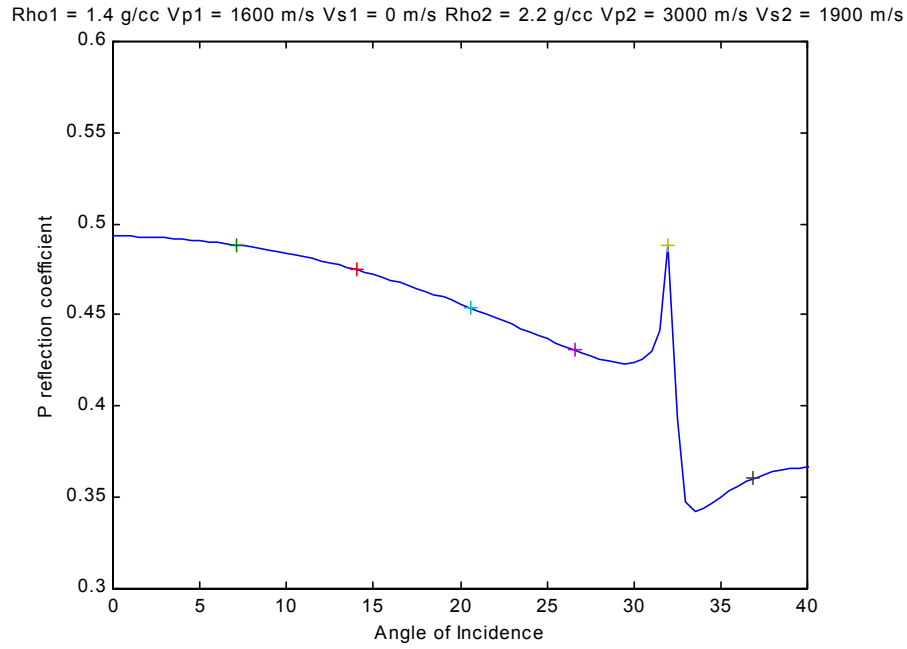


Figure 6. P reflection coefficients for a fluid with $V_{P1} = 1600$ m/s, $V_{S1} = 0$ m/s, $\rho_1 = 1.4$ g/cm³ and solid $V_{P2} = 3000$ m/s, $V_{S2} = 1900$ m/s, $\rho_2 = 2.2$ g/cm³.

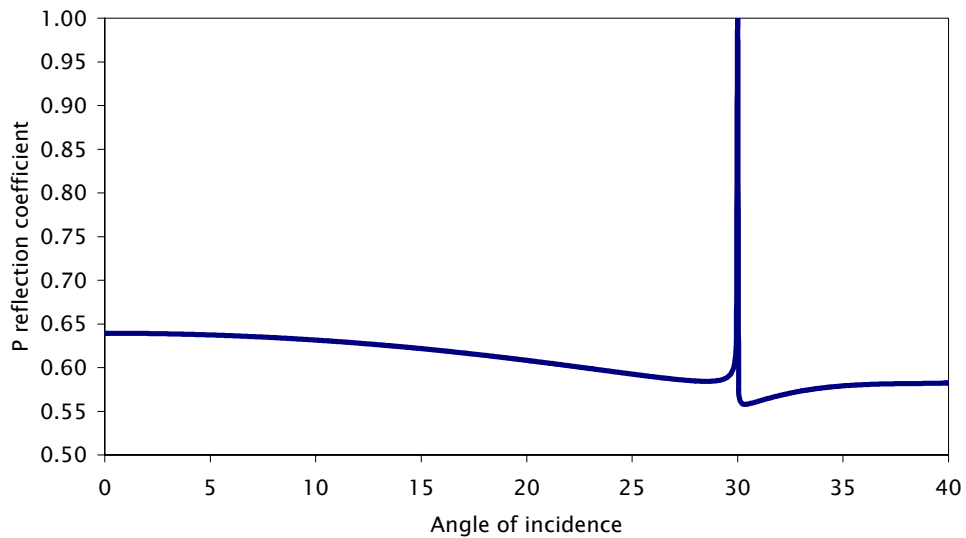


Figure 7a. P reflection coefficients for a fluid with $V_{P1} = 1500$ m/s, $V_{S1} = 0$ m/s, $\rho_1 = 1.1$ g/cm³ and solid $V_{P2} = 3000$ m/s, $V_{S2} = 2000$ m/s, $\rho_2 = 2.5$ g/cm³ (courtesy of Pat Daley).

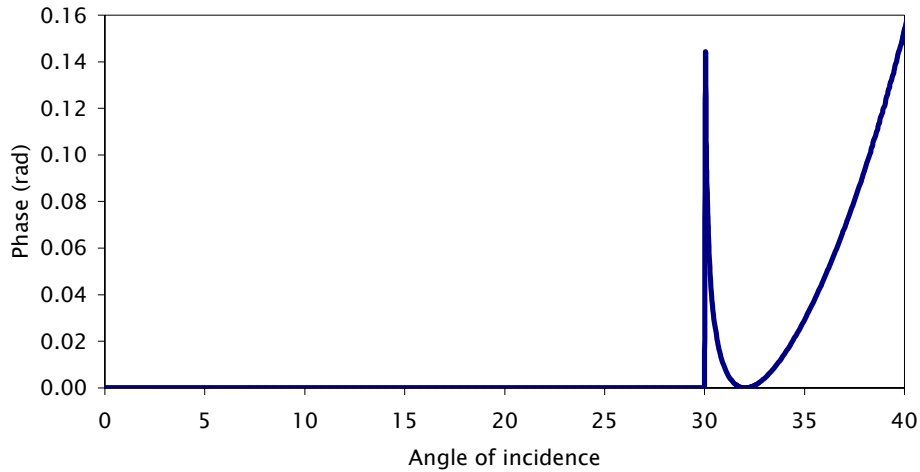


Figure 7b. Phase response for the reflection amplitudes in Figure 7a for a fluid with $V_{P1} = 1500$ m/s, $V_{S1} = 0$ m/s, $\rho_1 = 1.1$ g/cm³ and solid $V_{P2} = 3000$ m/s, $V_{S2} = 2000$ m/s, $\rho_2 = 2.5$ g/cm³ (courtesy of Pat Daley).

To design the geometry of the tool, we analysed the receiver aperture, separation from borehole wall, interval between receivers, and angles of incidence obtained for different situations. To calculate the angles of incidence from a specific configuration of the tool, i.e. a value for the receiver separation, and a value for the separation from the borehole wall we use the geometrical relation as in Figure 3. One example for a tool-borehole separation is shown below (Figure 8).

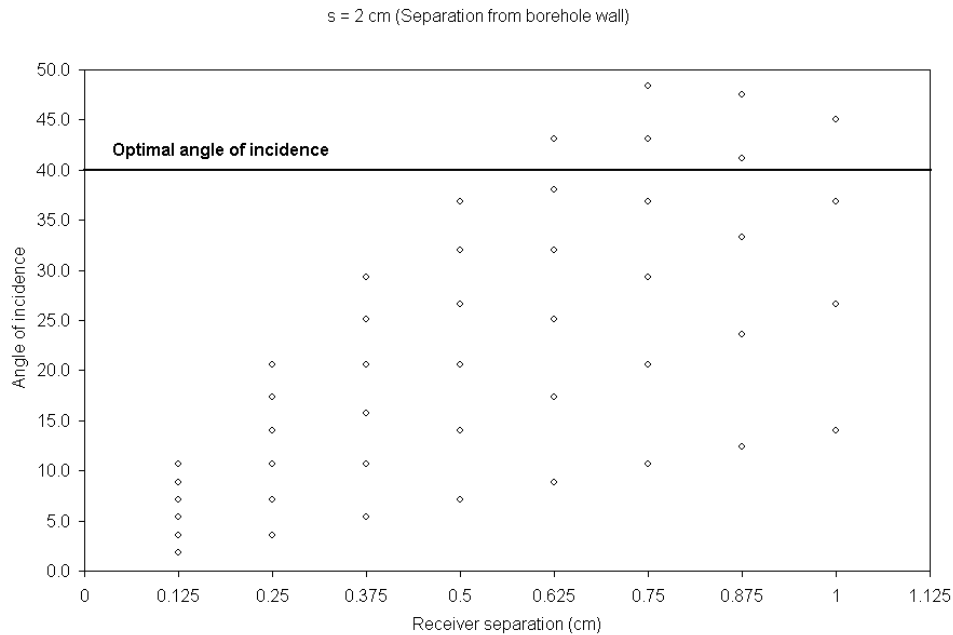


Figure 8. Determining the optimal separation between receivers for a tool-wall separation of 2cm.

Note that for greater redundancy we could use sources at either end of the receivers (Figure 9). In addition, we might be able to position the receivers orthogonally to the vertical array. That is, circumferentially around the cylinder shown in Figure 9. This might allow an orthogonal measurement of the reflectivity versus offset and thus the possibility of anisotropy determination.

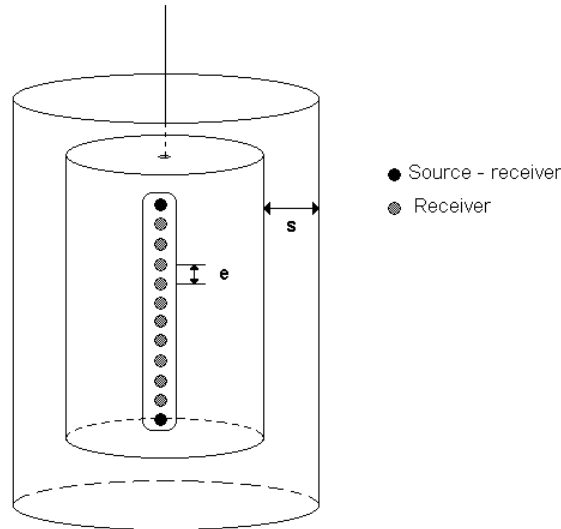


Figure 9. Schematic diagram of an elastic imaging tool with a source at either end of the receiving array.

ANALYSIS

From the AVO response of the reflected arrivals, we can begin to determine rock properties. First, from the increased reflectivity, we find the offset (and angle) at which critical reflection occurs. Then, from Snell's law and the fluid velocity, we know that:

$$V_{P2} = \frac{V_{P1}}{\sin \theta_{crit}}$$

We then use these velocities and an AVO relationship, such as that of Shuey (1985), we could determine the Poisson's ratio of the solid and thus an S-wave velocity.

CONCLUSIONS

We conclude that there is an AVO effect evident in simple models of an acoustic reflection in a fluid-filled borehole. An enhanced borehole imaging tool could be designed to capture this AVO information. From the critical angle amplitude anomaly and knowing the fluid velocity, we can determine the P-wave velocity of the formation. From the AVO variation, we could infer the S-wave velocity of the formation from standard AVO analysis techniques.

REFERENCES

- Daley, P.F., and Hron F. 1977, Reflection and transmission coefficients for transversely isotropic media: Bull., Seis. Soc. Am. **67**, 661-675.
- Graebner, M. 1992: Plane-wave reflection coefficient for a transversely isotropic solid. Geophysics, **57**, 1512-1519.
- Sheriff, R. and Geldart, L., 1989, 2nd Ed., Exploration Seismology: Cambridge University Press.
- Shuey, R.T., 1985, A simplification to the Zoeppritz equations. Geophysics, **50**, 609-614.